6

Spacecraft collision warning and avoidance strategy

Spacecraft collision warning and avoidance strategy is closely related to the detection capability and tracking efficiency of early warning systems. Theoretically, spacecraft collision warning and avoidance strategy can be very simple: what is needed is only a minimum approaching distance threshold. If the distance between the spacecraft and the space object is within the threshold, then avoidance maneuver is needed, otherwise, the spacecraft will be safe. However, to satisfy the abovementioned situation, detection system should meet the following three conditions: (1) a reasonable distributed detection system network able to track all passes and orbits of all space objects could be calculated without any error; (2) orbit dynamics model is accurate enough that the orbit prediction precision over 1 week would be 10 m or better, with no error divergence; and (3) there is no need to consider fuel consumption cost, orbit control time, and spacecraft effective working time and life span. Obviously, to meet the abovementioned three conditions is unrealistic.

Facing with tens of thousands of space objects, based on current technology, the above conditions could not be satisfied even using up global detection resources. Therefore in engineering, in order to carry out high accurate spacecraft collision warning analytical work, a kind of reasonable and feasible collision warning and avoidance strategy must be drawn up.

In fact, collision warning and avoidance strategy is the unification of the coordination between the capacity and accuracy of the entire detection resources as well as the spacecraft capacity of emergency response and feasible countermeasures. In spacecraft engineering, a successful and implementable collision warning strategy should meet the following three principles: (1) no missing alarm and fewer false alarms, (2) no interference to spacecraft routine work, and (3) sufficient time for avoidance maneuver with the lowest consumption.

In order to maintain the catalog integrity of tens of thousands space objects, the detection resources should be distributed averagely so that at least one pass of tracking data of each object (especial LEO object) can be obtained within 24 hours. As illustrated in Section 3.5, based on 2−3 minutes of moderate-precision radar measurement data per day, the orbit precision of cataloged space objects could be at the kilometer level, the 24-hour propagated orbit precision could be at 10-km level, and the 7-day propagated orbit precision could be at 100-km level. This is the common capacity of detection resources in the world. Using the abovementioned orbit determination and orbit prediction for collision warning, there must be a large number of false alarms. If the latter is applied in engineering for spacecraft avoidance, a great quantity of useless maneuvers of spacecraft and lots of unnecessary fuel consumption will be inevitable. Ultimately, the collision warning work loses its engineering

Spacecraft Collision Avoidance Technology. DOI: https://doi.org/10.1016/B978-0-12-818011-2.00006-4

value. Accordingly, the accuracy of orbit determination and orbit perdition becomes the key factor of the engineering feasibility of collision warning.

By using the measuring data of 1 day (or more) collected by global detection resources, the orbit precision of a space object can be more accurate than 10 m (see Section 3.5). However, considering the error of atmospheric model (particularly in Section 4.5), the orbit prediction precision in 24 hours could be several hundred meters, and that in 7 days could be 10 km. Therefore the collision warning based on orbit prediction of 100 m is the best means that current technology can achieve. To complete the orbit determination and prediction with the accuracy of 100 m of a space object, 1−2 days are needed in engineering. Considering the preparation for orbit control, a complete and feasible cycle of orbit measurement, prediction, early warning, and avoidance control will take 2−3 days, generally. Though it is not feasible for detection resources to make precision orbit determination and collision warning of all space objects in 3 days, it can be done if only for a few potential objects that really might be risky for collision. This chapter will discuss the following issues: how to select reasonable objects for precision orbit determination and collision warning with no missing alarm in 3 days ahead, as well as how to exclude false alarms and improve the reliability of early warning after precise orbit determination.

6.1 Collision warning calculation

There are two methods for space object collision warning: the minimum distance method (Box method) and the method based on probability of collision (Pc method). The minimum distance method is a kind of average method. NASA is the first one who adopted the method. If a space object enters the box area of 5 km × 25 km × 5 km in RTN direction (radial, tangential, normal to the orbital plane), the object will be monitored with special attention. If the object enters the box area of 2 km × 5 km × 2 km in RTN direction according to the calculation based on the latest orbit parameters, the decision on whether to perform avoidance maneuvers in action should be made combined with actual situations. However, the method does not consider the uncertainties of object position and geometry, resulting in high false alarm rate. Therefore scholars later proposed the probability of collision method for early warning. In fact, both methods have limitations. Nevertheless, according to the different features of objects and prediction duration, to carry out a comprehensive work of risk object screening, early warning and avoidance maneuvers based on the combination of the two methods may achieve success both theoretically and in engineering.

6.1.1 Risky object screening

The total number of measurable on-orbit space objects currently is around 16,000. The present available detection resources cannot afford to track and calculate orbits of all objects, and the calculation is unimaginable too. In order to reduce workload and improve computation efficiency, approaching analysis and risky object screening need to be done. In other words, before orbit prediction, the large amount of objects that will never collide with a

spacecraft needs to be removed first. The objects that might collide with the spacecraft and are within a certain distance to the spacecraft should be picked out for further orbit calculation and error analysis.

6.1.1.1 Screening by perigee and apogee

In order to find objects that might collide with the spacecraft in a short time, the initial screening of large quantities of space objects is needed. The first criterion is perigee and apogee. The objects whose perigee is greater than the spacecraft apogee and the objects whose apogee is smaller than the spacecraft perigee are removed. Further analysis will be made to the remaining objects.

Changes in perigee and apogee are mainly manifested in two aspects: one is the change in short term and the other is long term.

6.1.1.1.1 Short-term change of perigee

According to the basic theoretical knowledge of space object orbit, it is found that perigee can be expressed as:

$$H_p = a(1-e) = (\overline{a} + a_s^{(1)})(1 - \overline{e} + e_s^{(1)}) = \overline{a}(1-\overline{e}) + \overline{a}e_s^{(1)} + a_s^{(1)}(1-\overline{e}) + a_s^{(1)}e_s^{(1)}. \tag{6.1}$$

where H_p, a, and e are, respectively, the instantaneous perigee, semimajor axis, and eccentricity of the space object; $\overline{a}$ and $\overline{e}$ are, respectively, the mean semimajor axis and mean eccentricity; while $a_s^{(1)}$ and $e_s^{(1)}$ are, respectively, the first-order, short-term items of the mean semimajor axis and mean eccentricity. For space objects the perigee change is mainly decided by two items in the middle of formula Eq. (6.1). Based on the orbit characteristic, the change of $\overline{a}e_s^{(1)}$ is within 10 km, and the change of $a_s^{(1)}(1-\overline{e})$ is relevant with J_2 by 10^{-3}, which is usually within 10 km too. Therefore according to the characteristics of space object, it can be estimated that the change of perigee is generally about 10 km.

The change of apogee is similar to the change of perigee in short term.

6.1.1.1.2 Long-term change of perigee

As for LEO space object, the long-term change of its perigee is mainly influenced by atmospheric effects, resulting in decrease of perigee. The relationship between semimajor axis attenuation (m/ring) and atmospheric density, surface-to-mass ratio, and the semimajor axis is [3]:

$$da = -2\pi C_D \frac{S}{M}\rho a^2 \tag{6.2}$$

where C_D is the coefficient of atmospheric drag, S/M is the surface-to-mass ratio, and ρ is the atmospheric density.

According to the abovementioned formula and historical experience, the perigee change in 24 hours is within a few 100 m.

The change of apogee is similar to the change of perigee in long term.

Based on the abovementioned short-term and long-term changes, the estimation of space orbit is generally about a dozen kilometers, or up to 20 km.

6.1.1.1.3 Calculation and analysis of space object orbit change

To support the abovementioned theoretical analysis and estimation results, some actual satellite data are calculated. The change of perigee is shown from Figs. 6−1 to 6−4.

6.1.1.2 Screening by the geocentric distance of intersection

The second criterion is the geocentric distance of intersection. For two objects on two orbital planes, as long as the inclination or right ascension of the two objects is not equal, there will be two intersection points theoretically. The two objects might collide with each other only at the intersection points, so the geocentric distance of intersection becomes an important reference for the screening for risk objects, too. Space targets are screened according to the intersection geocentric distance, leaving targets that may pose a threat to spacecraft on-orbit for further analysis.

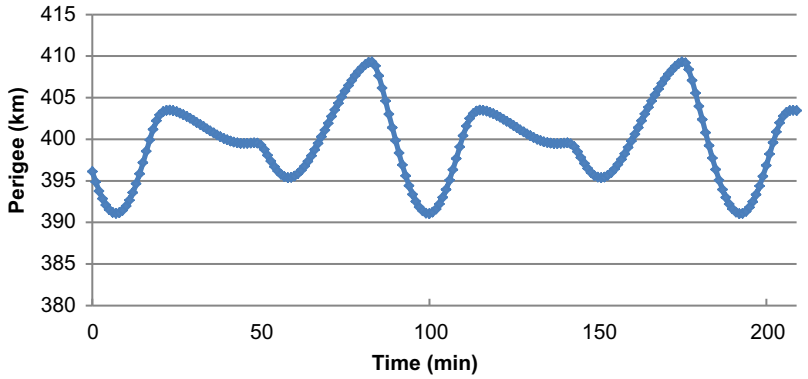

FIGURE 6–1 The perigee variation of object 25544 (H_a = 410 km, H_p = 401 km).

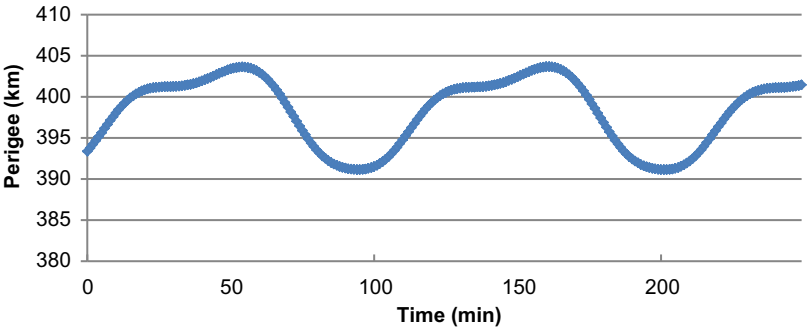

FIGURE 6–2 The perigee variation of object 21393 (H_a = 1765 km, H_p = 398 km).

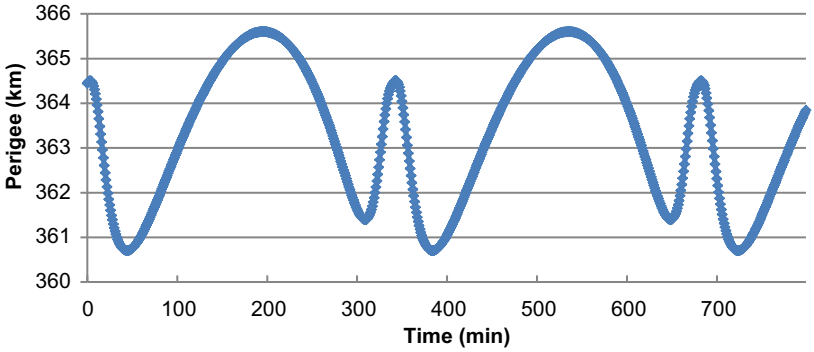

FIGURE 6–3 The perigee variation of object 28920 (H_a = 19,126 km, H_p = 361 km).

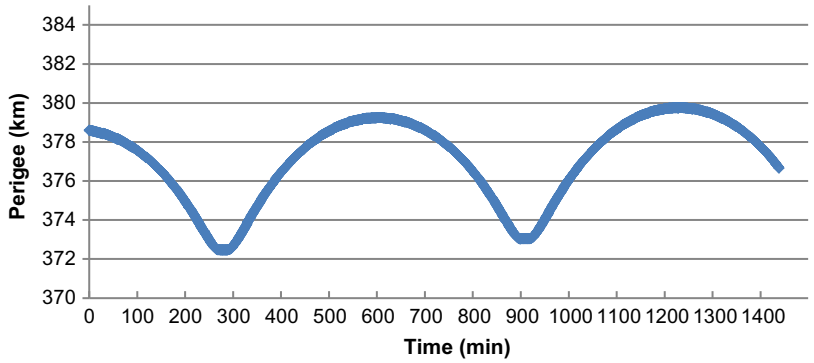

FIGURE 6–4 The perigee variation of object 39774 (H_a = 35,513 km, H_p = 372 km).

As shown in Fig. 6−5, i_0 and i_1 refer to the inclination of the spacecraft and orbit debris; A and B refer to orbit ascending node; C refers to the intersection of orbital planes; Θ refers to the intersection angle; $\widehat{AB}$ refers to the difference of ascending node $\Delta\Omega$; $\widehat{AC}$ refers to the arc u_0 from the spacecraft to the ascending node; and $\widehat{BC}$ refers to the arc u_1 from the ascending node to the intersection. It can be obtained the following:

$$\cos\theta = \cos i_1 \cos i_0 + \sin i_1 \sin i_0 \cos\Delta\Omega \tag{6.3}$$

$$\sin u_1 = \frac{\sin\Delta\Omega}{\sin\theta}\sin i_1 \tag{6.4}$$

$$\sin u_0 = \frac{\sin\Delta\Omega}{\sin\theta}\sin i_0 \tag{6.5}$$

By using the abovementioned formula, u_0 u_1 can be calculated and then the geocentric distance of intersection r_0 r_1 can be obtained. According to the geocentric distance of intersection, the space objects whose $|r_0 - r_1| > \Delta d$ can be removed.

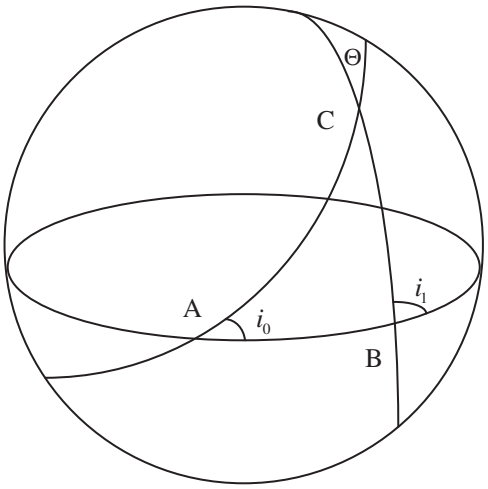

FIGURE 6–5 The celestial sphere diagram of satellites and debris.

When calculating the geocentric distance between two objects, the time difference between the two objects crossing the intersection point can be calculated simultaneously. However, as the two-body model is adopted in the calculation, using the time difference as a screening criteria will lead to a high false dismissal rate in practical engineering, thus it is often discarded.

6.1.1.3 Screening by the minimum distance between orbital planes

The third criterion is the minimum distance between two orbital planes. According to the criterion, the objects that may pose a threat to the spacecraft are picked out for further analysis.

The screening by the minimum distance between two orbital planes considers the geometry relationship of the two orbital planes. The intersection of two orbital planes is shown in Fig. 6—6.

For two elliptical orbits, there must be two closest distance d_1 and d_2, which are near the intersection line. d_1 and d_2 are called the minimum distance between two orbital planes. If the minimum distance between two orbital planes is greater than the threshold D, then there would be no possibility of collision for the two objects. Since the calculation of d_1 and d_2 is narrated in Ref. [107], herein it is omitted.

The three methods introduced here do not need detailed orbital calculation, but only qualitative judgment using four slow-varying parameters a,e,i, and Ω in the six elements of orbit. As long as one of the methods is used, the target whose orbit satisfies any one of the conditions will not collide with the primary target. Thus the calculation workload can be reduced by an order of magnitude with the minimum amount of computation and the fastest speed.

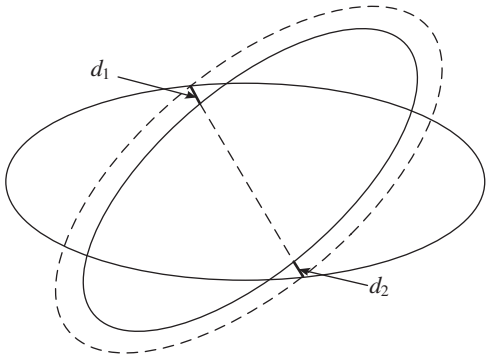

FIGURE 6–6 Screening by the minimum distance between two orbital planes.

6.1.2 The minimum distance calculation

The minimum distance and related parameters of two approaching objects is one of the important factors to determine whether there is a risk of collision. Neglecting the orbit prediction error, the factor becomes crucial for collision possibility calculation. Parameters involved in the minimum distance method includes the minimum distance between two objects, the distance component in UNW (or RTN) direction, the approaching velocity, the approaching angle, etc.

6.1.2.1 The minimum distance

For the relative minimum distance between two space objects, the main factor affecting the accuracy of the result is orbit propagation precision. Therefore for relevant objects, high-precision dynamic model should be adopted to make orbit extrapolation calculation. The method mainly consists of three parts that are discussed in the following subsections.

6.1.2.1.1 Space object orbit propagation

The dynamic model of space object orbit propagation is

$$\ddot{\mathbf{r}} = \mathbf{a}_0 + \mathbf{a}_\varepsilon \tag{6.6}$$

$$\mathbf{a}_0 = -\frac{GM_e}{r^3}\mathbf{r} \tag{6.7}$$

$$\mathbf{a}_\varepsilon = \sum_{i=1}^{6} \mathbf{a}_i \tag{6.8}$$

where G refers to Earth gravitational constant, $\mathbf{a}_0$ refers to the gravity acceleration of the center of the particle earth, and $\mathbf{a}_\varepsilon$ refers to the total perturbation acceleration. The involving perturbation models are as follows: Earth nonspherical perturbation, the third-body

perturbation, atmospheric damping perturbation, solar radiation pressure, earth tide, tidal perturbation, and relativistic effects.

6.1.2.1.2 The minimum distance calculation

Suppose the spacecraft position vector is $\mathbf{r}_1 = (\,x_1 \quad y_1 \quad z_1\,)^T$, the space object position vector is $\mathbf{r}_2 = (\,x_2 \quad y_2 \quad z_2\,)^T$, then the relative distance of the two objects is

$$D = \sqrt{(x_1 - x_2)^2 + (y_1 - y_2)^2 + (z_1 - z_2)^2} \tag{6.9}$$

The relative distance at all epoch between the spacecraft and the space object can be obtained, and then find the minimum one among them.

6.1.2.1.3 The relationship between relative velocity and relative distance at minimum distance

In J2000 geocentric inertial coordinate system, suppose the position vectors of the spacecraft and the space object are, respectively, $\mathbf{r}_1$ and $\mathbf{r}_2$; the velocity vectors of the spacecraft and the space object are, respectively, $\mathbf{v}_1$ and $\mathbf{v}_2$; and then the relative distance vector between the two will be

$$\Delta\mathbf{r} = \mathbf{r}_1 - \mathbf{r}_2 \tag{6.10}$$

Then the approaching velocity between the two will be

$$\Delta\mathbf{v} = \mathbf{v}_1 - \mathbf{v}_2 \tag{6.11}$$

The square of the relative distance vector will be

$$|\Delta\mathbf{r}|^2 = (\mathbf{r}_1 - \mathbf{r}_2) \cdot (\mathbf{r}_1 - \mathbf{r}_2) \tag{6.12}$$

Since now the minimum distance is achieved, then

$$\frac{\mathrm{d}|\Delta\mathbf{r}|^2}{\mathrm{d}t} = 2(\mathbf{r}_1 - \mathbf{r}_2) \cdot \frac{\mathrm{d}(\mathbf{r}_1 - \mathbf{r}_2)}{\mathrm{d}t} = 2(\mathbf{r}_1 - \mathbf{r}_2) \cdot (\mathbf{v}_1 - \mathbf{v}_2) = 0 \tag{6.13}$$

It can be obtained that

$$\Delta\mathbf{r} \cdot \Delta\mathbf{v} = 0 \tag{6.14}$$

This indicates that when the distance is the minimum, the relative position vector is perpendicular to the relative velocity vector. This feature can be used as a modified formula for iterative calculation of the nearest distance and greatly improves the calculation efficiency and accuracy.

6.1.2.2 The distance calculation in three directions

In order to describe the approaching of two space objects, besides the minimum distance, the distance components in three directions in UNW (or RTN) coordinate are also used.

In J2000 geocentric inertial coordinate system, suppose the position vectors of the spacecraft and space object at the minimum distance are $\mathbf{r}_1$ and $\mathbf{r}_2$, the relative distance between two objects will be

$$\Delta\mathbf{r} = \mathbf{r}_1 - \mathbf{r}_2 \tag{6.15}$$

Then in UNW coordinate system with the center of mass of the spacecraft as the origin, the distance components of the minimum distance in three directions are

$$\Delta\mathbf{r}_{\mathrm{UNW}} = \mathbf{M}_{\mathrm{UNW}} \cdot \Delta\mathbf{r} \tag{6.16}$$

where $\mathbf{M}_{\mathrm{UNW}}$ represents the transformation matrix from J2000 inertial coordinate system to UNW coordinate system.

Then in RTN coordinate system with the center of mass of the spacecraft as the origin, the distance components of the minimum distance in three directions are

$$\Delta\mathbf{r}_{\mathrm{RTN}} = \mathbf{M}_{\mathrm{RTN}} \cdot \Delta\mathbf{r} \tag{6.17}$$

where $\mathbf{M}_{\mathrm{RTN}}$ represents the transformation matrix from J2000 inertial coordinate system to RTN coordinate system.

6.1.2.3 The precision evaluation of three distance components

Among all thresholds in collision warning, the distance threshold is mainly relevant to the error of orbit prediction, which is determined by orbit determination error and prediction models. The orbit determination error is decided by the quality and number of data acquired by detection resources. Orbit prediction errors of different space objects are shown from Figs. 6−7 to 6−9.

According to Figs. 6−7 to 6−9 and the analysis in Section 5.2.4, the following conclusions for near-circular orbit objects are listed as follows:

1. The prediction error in radical and normal direction is relatively stable and is much smaller than that in tracking direction.
2. The prediction error is mainly in tracking direction, which is of rapid divergence over time. The lower the orbit altitude is, the more serious the divergence is. The perdition error in tracking direction is not of zero mean distribution. Instead, there is some systematical deviation; the prediction error is near the side of real trajectory.
3. The prediction error in radical direction is of divergence over time (but relative slowly) and systematical deviation. The lower the orbit altitude is, the more serious the divergence is.

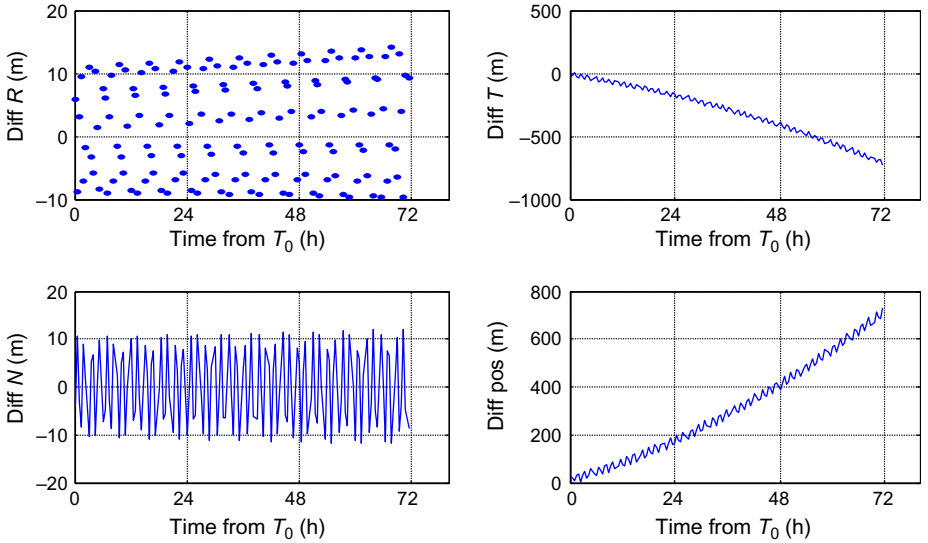

FIGURE 6–7 Orbit prediction error of object 1.

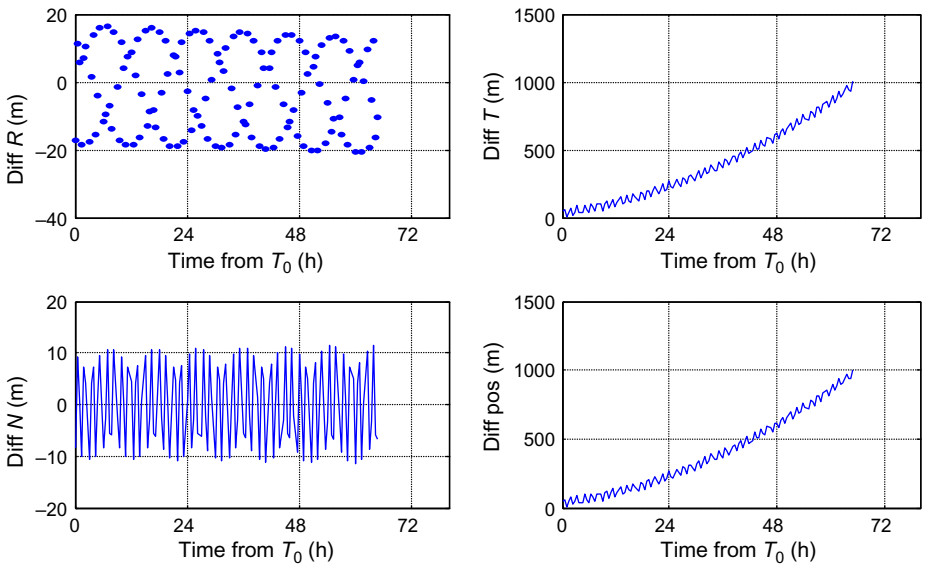

FIGURE 6–8 Orbit prediction error of object 2.

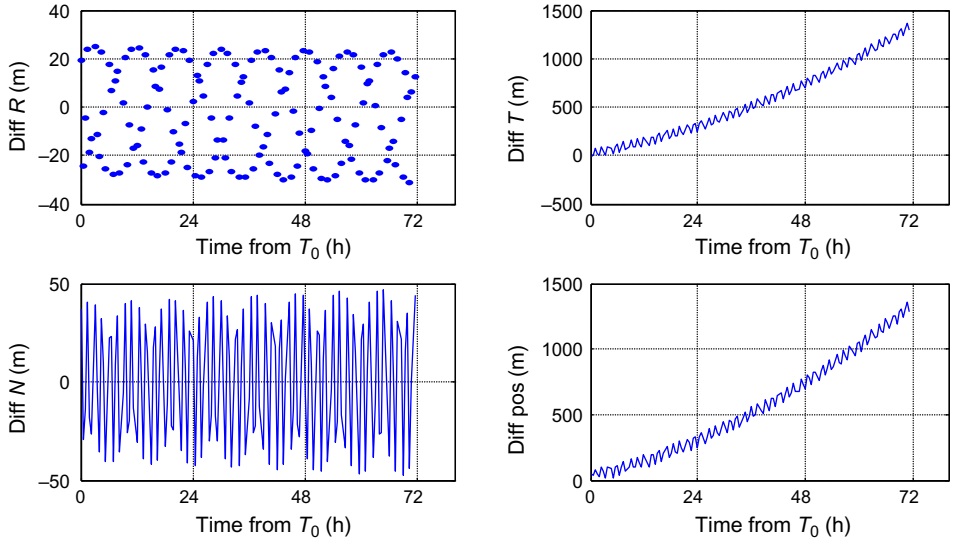

FIGURE 6–9 Orbit prediction error of object 3.

4. The prediction error in normal direction is smaller, most of which is under 100 m. Usually, it is of zero mean distribution, given nice measurement data constraint.

Therefore besides the minimum distance, radical distance is also considered to be an importance reference for collision warning threshold. Because the accuracy in radical and normal direction is much higher than that in tracking direction, by radical error, a great quantity of false alarms can be removed. If the velocity vectors of two objects at the approaching epoch are parallel or near parallel, normal error can also be used for removing false alarms.

6.1.2.4 Approaching angle and velocity calculation

In J2000 geocentric inertial coordinate system, suppose the position vectors of the spacecraft and space object are, respectively, $\mathbf{r}_1$ and $\mathbf{r}_2$; the velocity vectors of the spacecraft and space object are, respectively, $\mathbf{v}_1$ and $\mathbf{v}_2$; and then the approaching angle between the two objects will be

$$\theta = \arccos \frac{\mathbf{v}_1 \cdot \mathbf{v}_2}{|\mathbf{v}_1| \cdot |\mathbf{v}_2|} \tag{6.18}$$

Then the approaching velocity between the two objects will be

$$\Delta \mathbf{v} = |\mathbf{v}_1 - \mathbf{v}_2| \tag{6.19}$$

6.1.3 The probability of collision method

In space object collision risk analysis, the calculation of the probability of collision is one of the foundations. The probability of collision method adopts probability of collision as the index to describe collision risk degree. Probability of collision is defined as the probability of collision of two space objects, the position prediction of which is of errors. The calculation of probability of collision relies on the position, velocity, and the position covariance matrix information of spacecraft and space debris when they come across.

6.1.3.1 Probability of collision

Probability of collision is the probability when the distance between the center of objects is smaller than the combination of equivalent radius, which can be illustrated as $P_c = P(\rho < R)$ [107−109]. The distance between two objects is $\rho = |\boldsymbol{\rho}| = |\mathbf{r}_1 - \mathbf{r}_2|$. The actual position of two objects are $\mathbf{r}_1$ and $\mathbf{r}_2$, which can be expressed as the combination of the distribution center of two objects and a random error vector, that is, $\mathbf{r}_1 = \mathbf{r}_{1o} + \mathbf{e}_1$ and $\mathbf{r}_2 = \mathbf{r}_{2o} + \mathbf{e}_2$.

It is demonstrated in Section 6.1.2 that when the minimum distance between the two objects is achieved, the two objects are on a plane that is perpendicular to the relative velocity vector, and the plane is defined as the encounter plane. In this way the uncertainty of the position of two objects is allowed to be projected to the encounter plane so that the three-dimensional problem is simplified into a two-dimensional (2D) problem.

For the encounter plane, the function of probability of collision $f(x,z)$ and probability of collision P_c is calculated as the 2D Gaussian probability density function (PDF) is

$$f(x,z) = \frac{1}{2\pi\sigma_x'\sigma_z'}\exp\left[-\frac{1}{2}\left(\frac{(x-\mu_x)^2}{\sigma_x'2} + \frac{(z-\mu_z)^2}{\sigma_z'2}\right)\right] \tag{6.20}$$

where σ_x' and σ_z' are components of the error, while μ_x and μ_z are the distance components of the relative distance in the coordinate system of encounter plane. The probability of collision can be expressed as the integral of PDF in the circular domain:

$$P_c = \iint_{x^2+z^2 \le R^2} f(x,z)\mathrm{d}x\mathrm{d}z \tag{6.21}$$

The probability of collision results mainly contains the following items: object size, relative position, relative velocity, and position errors.

6.1.3.2 The maximum probability of collision

Theoretical and practical analysis show that, for a given intersection location, speed, geometry, and size of two objects, the probability of collision will increase with the increase of the position error uncertainty. Under certain conditions of the positional error, the probability of collision reaches the maximum, then the probability of collision decreases when the position error increases. In practical engineering applications the maximum probability of collision calculation is very important. Because the actual position error and the covariance matrix of

spacecraft and space object are generally unknown or only the shape without the specific size of the error ellipsoid is known, it is necessary to determine the probability of collision in the worst case. The maximum probability of collision can be also used for prescreening of space objects. When the maximum probability of collision is less than a threshold, it is supposed that the object will not pose a threat to spacecraft [101].

2D normal distribution PDF is as follows:

$$f(x,z)=\frac{1}{2\pi\sigma'_x\sigma'_z}\exp\left[-\frac{1}{2}\left(\frac{(x-\mu_x)^2}{\sigma'_x 2}+\frac{(z-\mu_z)^2}{\sigma'_z 2}\right)\right] \tag{6.22}$$

The probability of collision can be expressed as the integral of PDF in the circular domain:

$$P_c=\iint_{x^2+z^2\le R^2} f(x,z)\mathrm{d}x\mathrm{d}z \tag{6.23}$$

Because of the token independence of integral, the variable z is replaced by variable y in the following to be convenient. The unequal variance PDF is expressed as:

$$f(x,y)=\frac{1}{2\pi\sigma_x\sigma_y}\exp\left[-\frac{1}{2}\left(\frac{(x-\mu_x)^2}{\sigma_x^2}+\frac{\left(y-\mu_y\right)^2}{\sigma_y^2}\right)\right] \tag{6.24}$$

The probability of collision P_c is expressed as

$$P_c=\frac{1}{2\pi\sigma^2}\iint_{x^2+y^2\le R^2}\exp\left[-\frac{(x-\mu_x)^2+\left(y-\mu_y\right)^2}{2\sigma^2}\right]\mathrm{d}x\mathrm{d}y \tag{6.25}$$

Suppose

$$\mu_r=\sqrt{\mu_x^2+\mu_y^2} \tag{6.26}$$

Define dimensionless variable

$$v=\frac{\mu_r^2}{2\sigma^2},\quad u=\frac{R^2}{2\sigma^2} \tag{6.27}$$

Probability of collision P_c can be reduced to the form of infinite series. The first item is adopted as the approximation of P_c:

$$P_c=e^{-v}(1-e^{-u}) \tag{6.28}$$

In order to find the maximum of P_c, differentiate P_c of σ, and suppose the partial derivative is 0, then

$$\begin{aligned}\frac{\partial P_c}{\partial \sigma} &= \frac{\partial P_c}{\partial v}\frac{\partial v}{\partial \sigma} + \frac{\partial P_c}{\partial u}\frac{\partial u}{\partial \sigma} \\ &= e^{-v}(1-e^{-u})\frac{\mu_r^2}{\sigma^3} - e^{-v}e^{-u}\frac{R^2}{\sigma^3} = 0\end{aligned} \tag{6.29}$$

Rearranging the equation, we obtain

$$u = \ln\left(1 + \frac{R^2}{\mu_r^2}\right) \tag{6.30}$$

When P_c is the maximum, σ is

$$\sigma_D = \frac{R}{\sqrt{2\ln\left(1 + \left(R^2/\mu_r^2\right)\right)}} \tag{6.31}$$

The formula is substituted into the probability of collision of a first-order approximation expression, the maximum probability of collision $P_{c\max}$ is

$$P_{c\max} = \frac{R^2}{R^2 + \mu_r^2}\left(\frac{\mu_r^2}{R^2 + \mu_r^2}\right)^{\mu_r^2/R^2} \tag{6.32}$$

Define dimensionless variable

$$\lambda = \frac{\mu_r^2}{R^2} = \frac{v}{u} \tag{6.33}$$

Then the maximum probability of collision $P_{c\max}$ is

$$P_{c\max} = \frac{\lambda^\lambda}{(1+\lambda)^{1+\lambda}} \tag{6.34}$$

6.1.3.3 Influence of related parameters on probability of collision

Because there are errors in measurement and much uncertainty in orbit trajectory, in collision warning analysis, the influence of space motion (approaching distance, approaching angle), space orbit minimum distance, probability of collision, and other parameters must be considered. In space rendezvous determination, the influence factors and scales on collision warning need to be analyzed deeply.

The calculation of probability of collision comprehensively considers the geometry of rendezvous, the orbit prediction error, the size of object, and other factors, which is a comprehensive risk assessment index. However, in collision warning engineering, approaching

distance (and its UNW components), relative velocity, and rendezvous angle are important risk assessment indexes too. Under some situations, Box method based on UNW distance is more reliable, but more reliable indicates more conservative.

In such cases, it is necessary to understand the probability of collision, the UNW components of approaching distance, and their relationship in rendezvous geometry for further understanding of two indexes and their significance in reasonable application.

6.1.3.3.1 The Influence of distance and position error in *N* direction on probability of collision

According to the explicit formulation of probability of collision, probability of collision decreases with the distance increase in N direction. Fig. 6−10 shows the variation curve of probability of collision P_c with the distance change in N direction.

Fig. 6−11 shows P_c variation with the distance change in N direction too. However, its vertical coordinate axis is in logarithmic form. Fig. 6−11 shows that when $N > 2\text{ km} \approx 4\sigma_N$, $P_c < 10^{-8}$.

The influence of the overall position prediction error is the same with the influence in each direction in the following: the probability of collision P_c increases first and then decreases after reaching its maximum value. Suppose the distance in N direction changes and other conditions remain unchanged. Fig. 6−12 shows P_c variation with the distance error standard deviation variation in N direction. When $\sigma_N = 0.0315\text{ km} \approx N$, P_c reaches its maximum 2.966×10^{-4}.

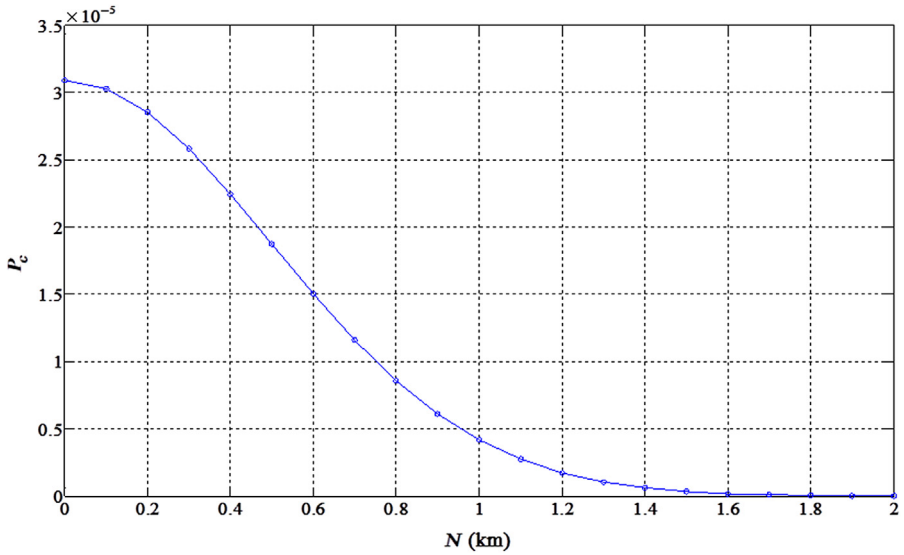

FIGURE 6–10 P_c variation with the distance change in N direction.

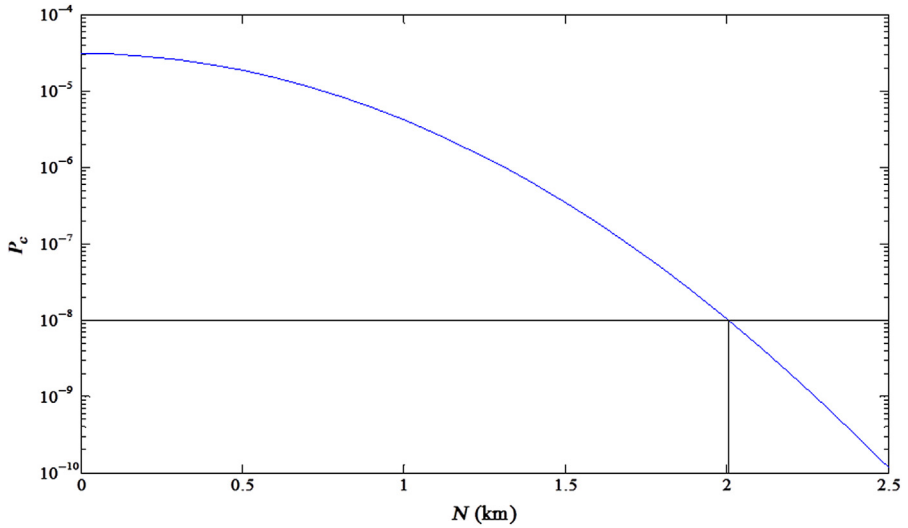

FIGURE 6–11 P_c variation with the distance change in N direction (vertical coordinate axis in logarithmic form).

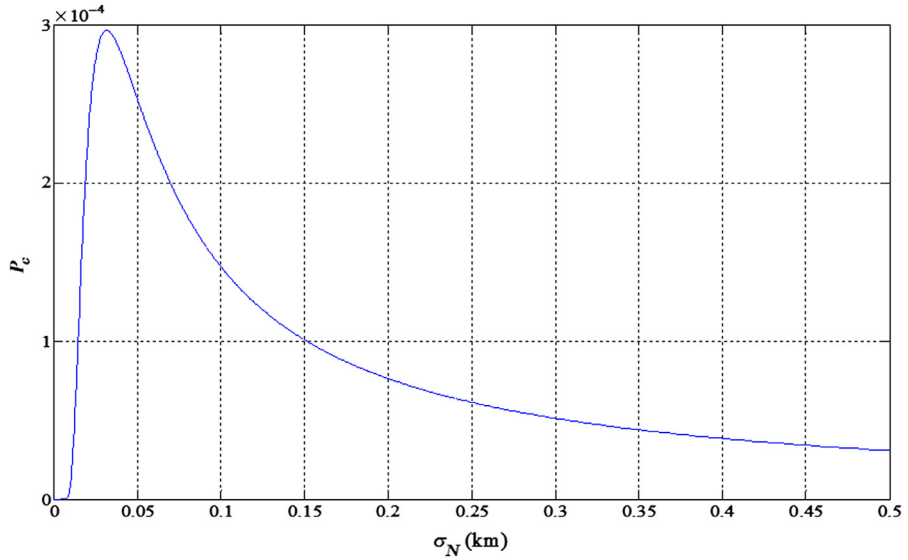

FIGURE 6–12 P_c variation with the distance error standard deviation variation in N direction.

6.1.3.3.2 The Influence of distance and position error in U and W direction on probability of collision

According to the explicit formulation of probability of collision, probability of collision decreases with the increase of the joint distance in U and W direction $\sqrt{U^2 + W^2}$. In the case where other conditions remain unchanged, Fig. 6−13 shows the variation of probability

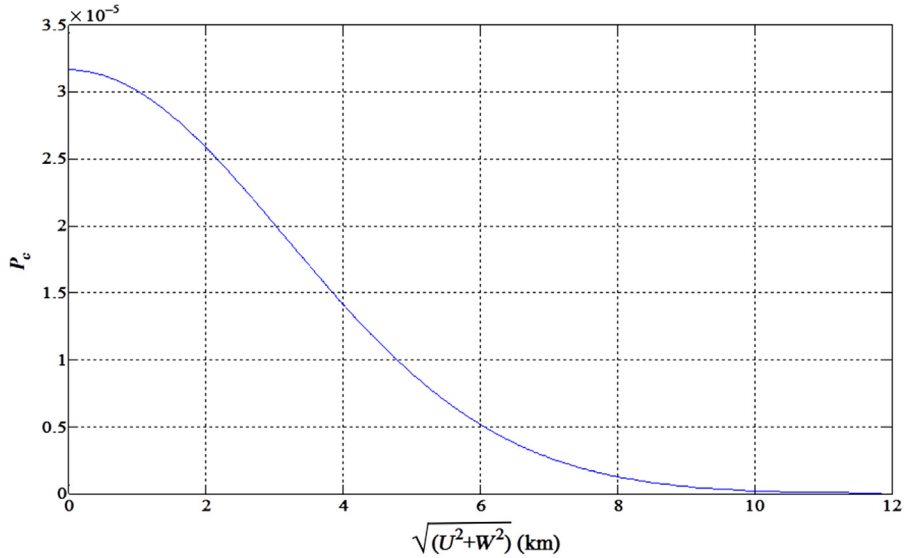

FIGURE 6–13 P_c variation with the change of $\sqrt{U^2+W^2}$.

of collision P_c with the change of $\sqrt{U^2+W^2}$. When $\sqrt{U^2+W^2} > 10\text{ km} \approx 3\sigma_{UW}$, P_c is already very small.

Suppose the error in U and W direction changes with the scale factor k, and other conditions remain unchanged. Fig. 6−14 shows the variation of probability of collision P_c with the change of k. When $k = 0.221$, that is, $\sigma_{UW} = 0.221 \times 3.1554 = 0.6973$ km, P_c reaches its maximum 8.678×10^{-5}.

6.1.3.3.3 The influence of approaching angle on probability of collision

The influence of orbital plane angle φ on probability of collision depends on the shape and the size of the joint error ellipsoid. In general, the prediction error in U direction is larger than that in W direction. At this time, with the orbital plane angle φ increasing from 0 to π, the joint error in U and W direction decreases. If the prediction error in U direction is greater than that in W direction, with the orbital plane angle φ increasing from 0 to π, the joint error in U and W direction increases. This result is derived by the following equation. The joint error variance on horizontal plane is

$$\sigma_{UW}^2 = \sigma_U^2 \cos^2\frac{\varphi}{2} + \sigma_W^2 \sin^2\frac{\varphi}{2} = \sigma_U^2 + \left(\sigma_W^2 - \sigma_U^2\right)\sin^2\frac{\varphi}{2} \tag{6.35}$$

When $\sigma_W^2 < \sigma_U^2$, σ_{UW}^2 decreases with the increase of φ in $[0, \pi]$; when $\sigma_W^2 > \sigma_U^2$, σ_{UW}^2 increases with the increase of φ in $[0, \pi]$.

In most cases where the orbital error is large, probability of collision decreases with the increase of error. When $\sigma_W^2 < \sigma_U^2$, probability of collision increases with the increase of φ in $[0, \pi]$; when $\sigma_W^2 > \sigma_U^2$, the probability of collision decreases with the increase of φ in $[0, \pi]$.

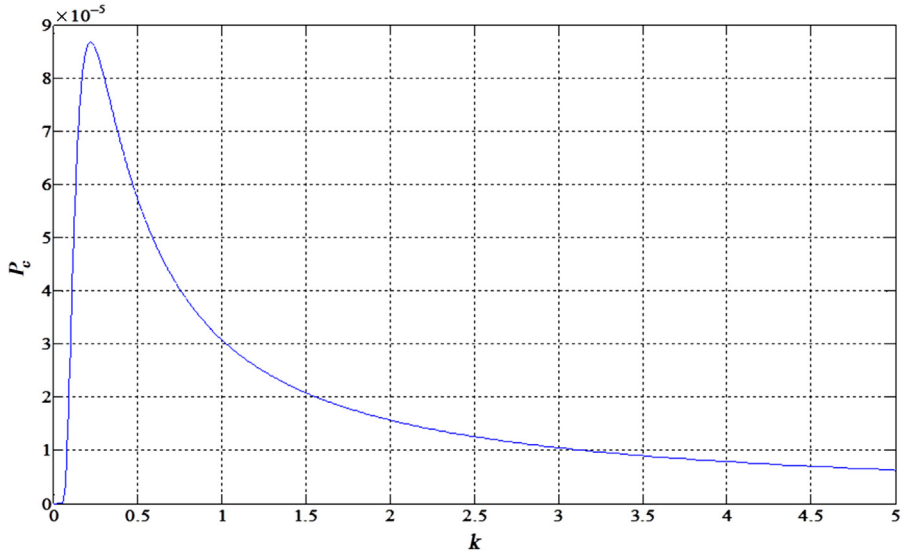

FIGURE 6–14 P_c variation with the change of k.

Fig. 6—15 shows P_c variation with the change of approaching angle. Because $\sigma_W^2 < \sigma_U^2$, σ_{UW}^2 decreases with the increase of φ, and the probability of collision increases first, and then decreases after reaching its maximum.

By analyzing the factors that affect probability of collision, we can get the following conclusions:

1. Because of the difference of the joint error ellipsoid shape, the impact of the angle between orbital planes on probability of collision is different. When the error in T direction is greater than that in N direction, the probability of collision increases with the increase of the angle between orbit planes; when the error in T direction is smaller than that in N direction, the probability of collision decreases with the increase of the angle between orbital planes. Generally, in position prediction, the error in T direction is always greater than that in R and N direction, so the probability of collision usually increases with the increase of the angle between orbital planes.
2. The influence of the overall position prediction error is the same with the influence in each direction in the following: the probability of collision increases first, and then decreases after reaching its maximum.

6.2 The method of spacecraft avoidance

On-orbit avoidance is an important measure for the safety of space mission. Collision avoidance maneuver is defined as to make sure that spacecraft do not collide with other space objects by orbit maneuvers based on comprehensive consideration of mission constraints

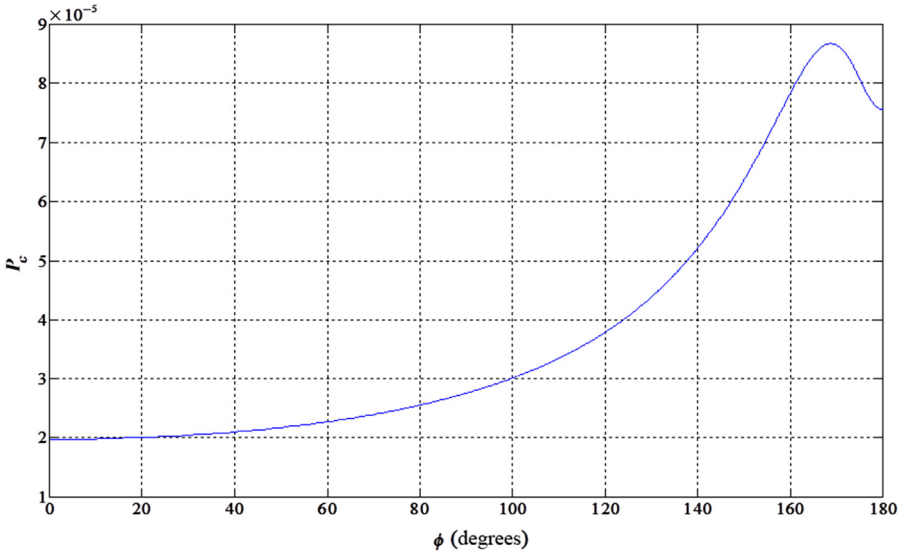

FIGURE 6–15 P_c variation with the change of approaching angle.

and orbit maintenance, according to the analysis of collision warning and information such as collision risk and geometric relation. Based on collision risk analysis, collision avoidance maneuver is able to give the guidelines and criteria of whether avoidance maneuver is needed, and the calculation methods and implementation strategies of optimal collision avoidance maneuvers, including the selection of direction and duration of thrust. Therefore avoidance maneuver is essentially a problem of orbit maneuvers, the essence of which is optimal transfer and mission constraints. In the choice for avoidance maneuver opportunity, spacecraft should be under the monitoring of tracking stations, and after orbit transfer, real-time measurement data could be obtained immediately so that the avoidance result can be evaluated. In calculation of speed increment the performance of spacecraft engine such as fuel and thrust needs to be considered too.

At present, many studies cast a light on impulse maneuvers for collision avoidance. According to the duration between rendezvous collision and orbit maneuvers, two collision avoidance strategies are offered: short-term and middle-term strategies. Short-term strategy is realized by altitude avoidance method. Since orbit prediction is made when collision is coming, a tangential velocity increment added by onetime pulse is adopted by this strategy so that the distance (radial distance) between the altitudes of two objects at the time when they approach each other is enlarged. Obviously, the required speed increment is greater. For middle-term strategy the method of separation in tracking direction is adopted. If there is still a long time before the rendezvous occurs, several small increments of velocity in tracking direction is then adopted so that the tangential distance between two objects at the approaching point will be increased. In other words, both the objects will encounter the intersection site, but they will be there in different time instead of simultaneously.

6.2.1 Altitude avoidance method

Altitude avoidance method is to pose a velocity increment along tracking direction during $n+1/2$ $(n=0,1,2,\ldots)$ orbit pass before potential collision, raising or lowering the altitude of spacecraft, and therefore when the spacecraft goes through the expected intersection site, there will be a radial distance from the risky object so as to avoid collision.

It is certain that at t_1, the spacecraft may collide with an object. It is required that within t_0, orbit maneuvers should be implemented, and because the potential collision is close to the maneuver time, altitude avoidance strategy is adopted. It can be seen that the key points of altitude avoidance are that the position and velocity of spacecraft at the time of maneuver and the object position are known, and orbit elements and velocity increment need to be calculated.

Suppose when no avoidance maneuver is taken, the spacecraft orbit is σ_0 and σ_1 at t_0 and t_1. If orbit maneuver is taken at t_0, then the spacecraft orbit is σ_0' and σ_1' at t_0 and t_1.

According to the theory of orbit motion and avoidance constraints, there are

$$\begin{aligned}
&\sigma_1 = \sigma_0 + \overline{\sigma_1}(t_1 - t_0) + \overline{\sigma_s}(t_1) - \overline{\sigma_s}(t_0)\\
&\sigma_1{}' = \sigma_0{}' + \overline{\sigma_1}'(t_1 - t_0) + \overline{\sigma_s}'(t_1) - \overline{\sigma_s}'(t_0)\\
&\sigma_0{}' = \sigma_0 + \Delta\sigma_0(\Delta v)\\
&r(\sigma_1{}') = r(\sigma_1) + \Delta r
\end{aligned} \tag{6.36}$$

where σ_0 and σ_1 are the instantaneous orbit elements at t_0 and t_1, $\overline{\sigma_1}$ and $\overline{\sigma_s}$ are the long-periodic and short-periodic coefficients of the orbit elements before the orbit changes; σ_0' and σ_1' are the instantaneous orbit element at t_0 after the orbit changes at t_0 and t_1; $\overline{\sigma_1}'$ and $\overline{\sigma_s}'$ are the long-periodic and short-periodic coefficients of the orbit elements after the orbit changes; $\Delta\sigma_0(\Delta v)$ represents the change of orbit elements caused by the speed variation after the orbit changes at t_0; and r is the position vector and Δr is the change of the position.

Because the energy consumption of orbit maneuver is small, the increment is small, too. Therefore $\Delta\sigma(\Delta a/a, \Delta e, \Delta i, \Delta\Omega, \Delta\omega, \Delta M)$ is generally of the amount of $O(10^{-3})$, and the difference between $\overline{\sigma_1}(\overline{\sigma_0})$ and $\overline{\sigma_1}'(\overline{\sigma_0}')$ is of $O\cdot(J_2\cdot\Delta\sigma_{a,e,i}) = O(10^{-6})$. Similarly, the difference between $\overline{\sigma_s}$ and $\overline{\sigma_s'}$ is of $O(10^{-6})$. Since the altitude avoidance method is often taken in emergency when the maneuver time and collision time is relatively close (no more than one cycle), there is $\Delta\sigma = (\overline{\sigma_1'} + \overline{\sigma_1})(t_1 - t_0) + (\overline{\sigma_s'}(t_1) - \overline{\sigma_s}(t_1)) - (\overline{\sigma_s'}(t_0) - \overline{\sigma_s}(t_0))$, which is about the magnitude of $O(10^{-5})$.

Based on the abovementioned analysis, in calculation of avoidance maneuver, two-body computation can be adopted. Lambert Flight Time Theory is adopted by this book for calculation. The calculation steps are as follows:

1. The iterative equation of semimajor axis a is obtained by the Lambert equation:

$$F(a) = n(t_2 - t_1) - ((\alpha - \sin\alpha) - (\beta - \sin\beta)) = 0 \tag{6.37}$$

The Newton iterative method is used for solving Eq. (6.37). Through Taylor expansion, it is estimated an initial value a_0, and only get to Δa,

$$F(a) = F(a_0) + \left(\frac{\mathrm{d}F}{\mathrm{d}a}\right)\Delta a = 0 \tag{6.38}$$

$$\frac{\mathrm{d}F}{\mathrm{d}a} = -\frac{3n}{2a}(t_2 - t_1) + \frac{r_1 + r_2 + c}{2a^2}\tan\frac{\alpha}{2} - \frac{r_1 + r_2 - c}{2a^2}\tan\frac{\beta}{2} \tag{6.39}$$

where $n = \sqrt{\mu/a^3}$

$$\begin{cases} \sin\dfrac{\alpha}{2} = \sqrt{\dfrac{r_1 + r_2 + c}{4a}} \\ \sin\dfrac{\beta}{2} = \sqrt{\dfrac{r_1 + r_2 - c}{4a}} \end{cases} \quad (0 \text{ degrees} < \beta < \alpha \le 180 \text{ degrees}) \tag{6.40}$$

$$c = |\vec{r}_1 - \vec{r}_2|$$

Δt_m is the time when the minimum energy ellipse flies from t_0 to t_1:

$$\Delta t_m = \sqrt{\frac{S^3}{2\mu}}\frac{\left[\alpha_m - \sin\alpha_m + (\beta_m - \sin\beta_m)\right]}{2} \tag{6.41}$$

In formula Eq. (6.41),

$$S = \frac{r_1 + r_2 + c}{2} \tag{6.42}$$

For the control problem where the geocentric distance r_1, r_2 and its angle Δf are known, the semimajor axis can be obtained based on the relationship between Δt and Δt_m, and the value of Δf:

$$\Delta t = t_2 - t_1 \tag{6.43}$$

$$\tan\Delta f = \frac{\mathbf{r}_2 \times \mathbf{r}_1}{\mathbf{r}_2 \cdot \mathbf{r}_1} \tag{6.44}$$

When $\Delta f \le 180$ degrees, $\Delta t \le \Delta t_m$

$$\begin{aligned} &F(a) = n(t_2 - t_1) - [(\alpha - \sin\alpha) - (\beta - \sin\beta)] \\ &\frac{\mathrm{d}F}{\mathrm{d}a} = -\frac{3n}{2a}(t_2 - t_1) + \left(\frac{r_1 + r_2 + c}{2a^2}\tan\frac{\alpha}{2} - \frac{r_1 + r_2 - c}{2a^2}\tan\frac{\beta}{2}\right) \end{aligned} \tag{6.45}$$

When $\Delta f \le 180$ degrees, $\Delta t \ge \Delta t_m$

$$\begin{aligned} &F(a) = n(t_2 - t_1) - [2\pi - (\alpha - \sin\alpha) - (\beta - \sin\beta)] \\ &\frac{\mathrm{d}F}{\mathrm{d}a} = -\frac{3n}{2a}(t_2 - t_1) - \left(\frac{r_1 + r_2 + c}{2a^2}\tan\frac{\alpha}{2} + \frac{r_1 + r_2 - c}{2a^2}\tan\frac{\beta}{2}\right) \end{aligned} \tag{6.46}$$

When $\Delta f \geq 180$ degrees, $\Delta t \leq \Delta t_m$

$$F(a) = n(t_2 - t_1) - [(\alpha - \sin\alpha) + (\beta - \sin\beta)]$$
$$\frac{\mathrm{d}F}{\mathrm{d}a} = -\frac{3n}{2a}(t_2 - t_1) + \left(\frac{r_1 + r_2 + c}{2a^2}\tan\frac{\alpha}{2} + \frac{r_1 + r_2 - c}{2a^2}\tan\frac{\beta}{2}\right) \tag{6.47}$$

When $\Delta f \geq 180$ degrees, $\Delta t \geq \Delta t_m$

$$F(a) = n(t_2 - t_1) - [2\pi - (\alpha - \sin\alpha) + (\beta - \sin\beta)]$$
$$\frac{\mathrm{d}F}{da} = -\frac{3n}{2a}(t_2 - t_1) - \left(\frac{r_1 + r_2 + c}{2a^2}\tan\frac{\alpha}{2} - \frac{r_1 + r_2 - c}{2a^2}\tan\frac{\beta}{2}\right) \tag{6.48}$$

Also because

$$\Delta a = -\frac{F(a_0)}{(\mathrm{d}F/\mathrm{d}a)_0} \tag{6.49}$$

Therefore the semimajor axis after avoidance is

$$a_1 = a_0 + \Delta a \tag{6.50}$$

2. Judge whether a_1 meets the accuracy requirement, namely, $|a_1 - a_0| \leq \varepsilon$. If not, Taylor expansion of $F(a)$ needs to be done at a_1. Do it repeatedly until the required accuracy of a is obtained.
3. For normal spacecraft, since the flight path is usually a circular orbit, the velocity increment of orbit maneuver can be expressed as:

$$\Delta v = v_2 - v_1 = \sqrt{\mu\left(\left(\frac{2}{r_1} - \frac{1}{a_2}\right) - \left(\frac{2}{r_1} - \frac{1}{a_1}\right)\right)} \tag{6.51}$$

This method uses Lambert Flight Principles, replacing the precision orbit prediction method by a simplified model of two-body Kepler. By the given constraints, the avoidance maneuver velocity increment is solved.

On this basis, combined with the 2D probability of collision integration method, using fixed-step searching method, the optimal solution of avoidance maneuver velocity increment can be obtained.

6.2.2 Time avoidance method

Time avoidance method is to pose several velocity increments along tracking direction during $n(n \geq 2)$ orbit passes before the potential collision, raising or lowering the altitude of spacecraft, and therefore the spacecraft will not go through the intersection site at the original time so as to avoid collision with risky object.

It can be seen that the key point of time avoidance is the calculation of the velocity increment at the maneuver point given the position and velocity of spacecraft at the time of maneuver and the object position. The steps of computation are as follows:

1. The orbital period before maneuver is

$$T_1 = \frac{2\pi}{\sqrt{\mu/a_1{}^3}} \tag{6.52}$$

2. According to the avoidance constraints, it is assumed that Δt_a needs to be staggered to the expected collision time, the orbital period after maneuver is

$$T_2 = T_1 + (-1)^j \Delta t_a / \frac{t_1 - t_2}{T_1} \qquad (j = 1, 2) \tag{6.53}$$

3. Thus the semimajor axis of the object orbit is

$$a_2 = \sqrt[3]{\frac{\mu}{(2\pi/T_2)^2}} \tag{6.54}$$

4. Therefore the orbit maneuver velocity increment can be expressed as

$$\Delta v = v_2 - v_1 = \sqrt{\mu\left[\left(\frac{2}{r_1} - \frac{1}{a_2}\right) - \left(\frac{2}{r_1} - \frac{1}{a_1}\right)\right]} \tag{6.55}$$

Directly by the relationship between orbit period and semimajor axis, and the given constraints, the desired velocity increment can be obtained.

On this basis, combined with the 2D probability of collision integration method, using fixed-step searching method, the optimal solution of velocity increment of the avoidance maneuver can be obtained.

6.3 Collision warning strategy for spacecraft safety operation and case studies

Due to the increasing utilization rate of space resources and increasing number of space objects, the orbit environment of spacecraft is deteriorating, and the probability of collision of space objects is growing. The destruction of any satellite will bring immeasurable loss to the national economy and national security. In order to protect the safety of space missions and reduce the costs by false alarms, it is necessary to formulate and improve organizational procedures and construct an integrated system of collision warning and avoidance.

According to the accuracy of orbit prediction and the desired time for avoidance measures, the procedures of spacecraft collision warning and avoidance are divided into four stages: risky objects screening, daily warning analysis, precision collision warning, and avoidance control.

6.3.1 Risky objects screening

Collision warning calculations of all on-orbit spacecraft in 7 days are carried out by normal cataloging orbit data every day. If there is any approaching event entering the risky threshold of collision warning, supplementary tracking plans will be added for those risky objects so as to accumulate measurement data for future judgment of risky degrees.

In order to verify the feasibility of the risky objects screening algorithm, a case study of nine on-orbit spacecraft with more than 15,000 space objects in space on August 21, 2014, is made. The first screening is made by the altitude of perigee and apogee. The second screening is made by the geocentric distance of intersection. The third screening is made by the minimum distance between orbital planes. The following is the results of eight different screening conditions.

Screening condition 1:

1. Perigee is lower than 20 km, and apogee is higher than 20 km.
2. The geocentric distance of intersection is 50 km.

Screening condition 2:

1. Perigee is lower than 20 km, and apogee is higher than 20 km.
2. The minimum distance between orbital planes is 50 km.

Screening condition 3:

1. Perigee is lower than 20 km, and apogee is higher than 20 km.
2. The geocentric distance of intersection is 20 km.

Screening condition 4:

1. Perigee is lower than 20 km, and apogee is higher than 20 km.
2. The minimum distance between orbital planes is 20 km.

Screening condition 5:

1. Perigee is lower than 40 km, and apogee is higher than 40 km.
2. The geocentric distance of intersection is 50 km.

Screening condition 6:

1. Perigee is lower than 40 km, and apogee is higher than 40 km.
2. The minimum distance between orbital planes is 50 km.

Screening condition 7:

1. Perigee is lower than 40 km, and apogee is higher than 40 km.
2. The geocentric distance of intersection is 20 km.

Screening condition 8:

1. Perigee is lower than 40 km, and apogee is higher than 40 km.
2. The minimum distance between orbital planes is 20 km.

The results show that:

1. Due to different distribution of the number of objects in different altitudes, the percentage of risky objects for under screening conditions increases first and then decreases with the increase of orbit altitude. According to the analysis in Tables 6−1 to 6−5, the results are influenced by the volume ratio of objects in different altitudes.
2. For the objects below 500 km the percentage of risky objects is about 10% by the screening of perigee and apogee; for the objects from 500 to 900 km, the percentage of risky objects is about 40% by the screening of perigee and apogee; for the objects above 900 km the percentage of risky objects is about 30% by the screening of perigee and apogee. To some extent the influence of the threshold in the screening by perigee and apogee is limited on the results. It is indicated that for the method of perigee and apogee screening, the precision requirements for rendezvous time and orbit prediction are not

Table 6–1 Approaching events screening (Screening condition 1).

				After first screening		After second screening	
Object	**Altitude (km)**	**Perigee (km)**	**Apogee (km)**	**Number**	**Percentage**	**Number**	**Percentage**
Satellite1	500 or less	367	377	620	4.1	144	1.0
Satellite2		473	492	1336	8.8	468	3.1
Satellite3	500−900	581	586	2256	14.8	1003	6.6
Satellite4		620	662	3561	23.4	1832	12.0
Satellite5		684	697	3849	25.3	2102	13.8
Satellite6		786	794	5346	35.2	3139	20.7
Satellite7		816	831	5967	39.3	3418	22.5
Satellite8	900 or more	981	1196	5025	33.1	1220	8.0
Satellite9		1190	1211	2628	17.3	466	3.1

Table 6–2 Approaching events screening (Screening condition 2).

				After first screening		After second screening	
Object	**Altitude (km)**	**Perigee (km)**	**Apogee (km)**	**Number**	**Percentage**	**Number**	**Percentage**
Satellite1	500 or less	367	377	620	4.1	146	1.0
Satellite2		473	492	1336	8.8	468	3.1
Satellite3	500−900	581	586	2256	14.8	1004	6.6
Satellite4		620	662	3561	23.4	1836	12.1
Satellite5		684	697	3849	25.3	2103	13.8
Satellite6		786	794	5346	35.2	3147	20.7
Satellite7		816	831	5967	39.3	3425	22.5
Satellite8	900 or more	981	1196	5025	33.1	1227	8.1
Satellite9		1190	1211	2628	17.3	472	3.1

Table 6–3 Approaching events screening (Screening condition 3).

				After first screening		After second screening	
Object	**Altitude (km)**	**Perigee (km)**	**Apogee (km)**	**Number**	**Percentage**	**Number**	**Percentage**
Satellite1	500 or less	367	377	620	4.1	79	0.5
Satellite2		473	492	1336	8.8	248	1.6
Satellite3	500–900	581	586	2256	14.8	542	3.6
Satellite4		620	662	3561	23.4	966	6.4
Satellite5		684	697	3849	25.3	1127	7.4
Satellite6		786	794	5346	35.2	1801	11.8
Satellite7		816	831	5967	39.3	1722	11.3
Satellite8	900 or more	981	1196	5025	33.1	503	3.3
Satellite9		1190	1211	2628	17.3	234	1.5

Table 6–4 Approaching events screening (Screening condition 4).

				After first screening		After second screening	
Object	**Altitude (km)**	**Perigee (km)**	**Apogee (km)**	**Number**	**Percentage**	**Number**	**Percentage**
Satellite1	500 or less	367	377	620	4.1	80	0.5
Satellite2		473	492	1336	8.8	248	1.6
Satellite3	500–900	581	586	2256	14.8	542	3.6
Satellite4		620	662	3561	23.4	966	6.4
Satellite5		684	697	3849	25.3	1129	7.4
Satellite6		786	794	5346	35.2	1807	11.9
Satellite7		816	831	5967	39.3	1726	11.3
Satellite8	900 or more	981	1196	5025	33.1	504	3.3
Satellite9		1190	1211	2628	17.3	235	1.6

Table 6–5 Approaching events screening (Screening condition 5).

				After first screening		After second screening	
Object	**Altitude (km)**	**Perigee (km)**	**Apogee (km)**	**Number**	**Percentage**	**Number**	**Percentage**
Satellite1	500 or less	367	377	721	4.8	180	1.2
Satellite2		473	492	1595	10.5	547	3.6
Satellite3	500–900	581	586	2713	17.8	1311	8.6
Satellite4		620	662	4078	26.9	2050	13.5
Satellite5		684	697	4512	29.7	2505	16.5
Satellite6		786	794	6340	41.8	3785	24.9
Satellite7		816	831	6859	45.2	4034	26.6
Satellite8	900 or more	981	1196	5462	36.0	1248	8.2
Satellite9		1190	1211	2784	18.3	518	3.4

high, and therefore the method is suitable for initial screening for long-term collision warning based on cataloging orbit data.

3. For the objects below 500 km the percentage of risky objects is about 5% by the screening of perigee and apogee combined with the geocentric distance of intersection or the minimum distance between orbital planes; for the objects from 500 to 900 km the percentage of risky objects is about 30% by the screening of perigee and apogee combined with the geocentric distance of intersection or the minimum distance between orbital planes; for the objects above 900 km the percentage of risky objects is about 15% by the screening of perigee and apogee combined with the geocentric distance of intersection or the minimum distance between orbital planes. The smaller the geocentric distance of intersections or the minimum distance between orbital planes is, the smaller the percentage is.
4. With the same screening conditions of perigee and apogee, the number of risky objects screened by the geocentric distance of intersection is smaller than that screened by the minimum distance between orbital planes. The screening by the geocentric distance of intersection may cause missing alarms. Therefore the minimum distance between orbital planes is better than the geocentric distance of intersection as a screening algorithm.
5. In actual warning calculation the screening condition of perigee and apogee is required to be larger than 20 km, the minimum distance between orbital planes is required to be larger than the warning threshold. It can be reasonably adjusted according to actual situation so as to ensure screening efficiency without missing alarms.
6. By using the perigee and apogee as well as the minimum distance between orbital planes as screening conditions, the object number that needs to be further calculated is lessened, shortening warning calculation duration and improving warning efficiency (Tables 6−6 and 6−7).

In the stage of risky objects screening, the screening thresholds are mainly related to the orbit shape of space object, including perigee, apogee, the geocentric distance of

Table 6–6 Approaching events screening (Screening condition 6).

				After first screening		After second screening	
Object	**Altitude (km)**	**Perigee (km)**	**Apogee (km)**	**Number**	**Percentage**	**Number**	**Percentage**
Satellite1	500 or less	367	377	721	4.8	182	1.2
Satellite2		473	492	1595	10.5	547	3.6
Satellite3	500−900	581	586	2713	17.8	1312	8.7
Satellite4		620	662	4078	26.9	2054	13.5
Satellite5		684	697	4512	29.7	2506	16.5
Satellite6		786	794	6340	41.8	3794	25.0
Satellite7		816	831	6859	45.2	4041	26.6
Satellite8	900 or more	981	1196	5462	36.0	1255	8.3
Satellite9		1190	1211	2784	18.3	524	3.5

Table 6–7 Approaching events screening (Screening condition 7).

				After first screening		After second screening	
Object	**Altitude (km)**	**Perigee (km)**	**Apogee (km)**	**Number**	**Percentage**	**Number**	**Percentage**
Satellite1	500 or less	367	377	721	4.8	79	0.5
Satellite2		473	492	1595	10.5	248	1.6
Satellite3	500–900	581	586	2713	17.8	542	3.6
Satellite4		620	662	4078	26.9	966	6.4
Satellite5		684	697	4512	29.7	1127	7.4
Satellite6		786	794	6340	41.8	1801	11.8
Satellite7		816	831	6859	45.2	1722	11.3
Satellite8	900 or more	981	1196	5462	36.0	503	3.3
Satellite9		1190	1211	2784	18.3	234	1.5

Table 6–8 Approaching events screening (Screening condition 8).

				After first screening		After second screening	
Object	**Altitude (km)**	**Perigee (km)**	**Apogee (km)**	**Number**	**Percentage**	**Number**	**Percentage**
Satellite1	500 or less	367	377	721	4.8	80	0.5
Satellite2		473	492	1595	10.5	248	1.6
Satellite3	500–900	581	586	2713	17.8	542	3.6
Satellite4		620	662	4078	26.9	966	6.4
Satellite5		684	697	4512	29.7	1129	7.4
Satellite6		786	794	6340	41.8	1807	11.9
Satellite7		816	831	6859	45.2	1726	11.4
Satellite8	900 or more	981	1196	5462	36.0	504	3.3
Satellite9		1190	1211	2784	18.3	235	1.6

intersection, and the minimum distance between orbital planes. These parameters are related to the semimajor axis a, the eccentricity e, right ascension of ascending node Ω, and the argument of perigee ω but have no relations to mean anomaly M, which is hard to predict. According to Section 5.2.4, in normal cataloging orbit prediction, the element M in tracking direction is hard to predict, the forecast error of which in 7 days reaches hundreds of kilometers, whereas the error of perigee and apogee in 7 days is less than 40 km, and the error of the minimum distance between orbital planes is less 20 km. Therefore based on cataloging orbit prediction and the threshold in Table 6–8, using perigee, apogee, and the minimum distance between two orbital planes to screen the potential risky rendezvous in the next 7 days, the number of objects that need attention can be lessened by 90% without missing alarms, leaving good conditions for further observation on remaining 10% risky objects and removing false alarms.

Two principles are obeyed in the risky object screening stage: (1) based on the current orbit cataloging, without adding detection resources, to screen risky objects that might collide with spacecraft in 7 days and (2) on the basis of no missing alarm, to reducing the number of risky objects so that detection resources can satisfy further observation needs.

6.3.2 Daily warning analysis

In the stage of daily warning analysis, the analysis on the risky objects in the future 7 days will be made every day, on the basis of maintaining orbit cataloging and current workload of detection network. Though the risky objects are reduced by 90% in the first stage, most of the remaining objects are still false alarms. According to the results, for a satellite in the orbit of 500−1000 km, there would be two-to-three potential collision warnings, most of which will not actually occur. False alarm rate is too high that if it is used as the guidance for spacecraft avoidance, normal work of spacecraft would be impossible, and high fuel consumption would shorten the life span of spacecraft sharply. However, objects that might cause real collision with very low probability are among those objects. We should identify them.

In order to find reliable information among the collision data with high false alarm rate, the remaining 10% risky objects should be further monitored by detection resources. However, the observation work of all remaining objects is still huge and impossible to complete. According to Table 3−1, for a space object lower than 500 km, by using tracking data of two passes of orbit ascension or descension, the 3-day orbit prediction accuracy will reach the order of kilometer, and the accuracy of orbit position in radical and normal directions will be 20−30 m. In this way the accuracy is improved by one-to-two magnitudes. From the day of risky objects screening that is 7 days ahead of potential collision to the day that is 3 days ahead of potential collision, there are still 3 days for detection network to adjust observation plans. At the moment, what need to do is only to add more observation of an ascension or descension orbit pass to the current tracking plans, which is the lowest adjustment for the plan. Using the additional 2−3 days tracking data, the orbit prediction could be of the order of kilometer, and the accuracy of orbit position in radical and normal direction could be 10 m, based on which high reliable collision analysis could be done by using reasonable distance thresholds.

The choice of thresholds for minimum distance method is related to the precision of detection resources, the size of space objects, the inclination and altitude of object orbit, the computation software accuracy and calculation time. In the process of risky object screening, due to the requirement of calculation accuracy and efficiency, the method of simple numerical orbit cataloging calculation proposed in this chapter is recommended for calculation. However, simple numerical orbit cataloging calculation, American two-line element calculation method, average elements orbit cataloging calculation and half-numerical and half-analysis orbit cataloging calculation all can be used for orbit calculation and collision warning in the stage of risky object screening. However, in the following stages, numerical method with high-precision models is recommended. Generally, the collision warning of risky objects in 3 days calculated by precision orbit method after screening by risky objects

screening stage and additional observation of two passes of orbit ascension or descension is defined as yellow warning.

On the basis of no false dismissals, yellow warning is of high credibility, lessening the probability of false alarms. The formulation of a proper threshold for yellow warning should ensure that the probability of false alarm is low enough that it has no influence on the life span and normal operation of spacecraft, and there will not be any false dismissals. According to the current number of space objects, the capability of detection network, and the comprehensive performance of spacecraft, there should be no more than three-to-five false alarms of yellow warning for each spacecraft every year.

6.3.3 Precision collision warning

When yellow warning is issued and risky objects are identified, in the next 48 hours, the countable risky objects will be observed and tracked by detection resources with concentration to acquire high-precision orbit data 24 hours before the potential collision. In the next 48 hours after yellow warning is released, five passes of orbit ascension and descension or at least two passes of orbit ascension and descension of precision observation data should be acquired by detection network. According to Table 3−1, based on two passes of tracking data, orbit prediction accuracy in 24 hours will reach the order of a 100 m, satisfying very basic collision warning analysis. Based on five passes of tracking data, orbit prediction accuracy in 24 hours will be within a 100 m, whose credibility is highly improved. The collision warning of objects that cannot be removed in this stage is called red warning.

The premise and foundation of accuracy improvement of orbit prediction is to acquire orbit measurement data as much as possible. Even for red warning, the accuracy of dynamic models, especially atmospheric drag models is a major factor that affects the precision of orbit prediction and the bottleneck of confidence level. In Section 4.5 the major four factors that affect the precision of atmospheric drag model are discussed in detail. The error of area−mass ratio of object, atmospheric density model, and average $F_{10.7}$ value in 81 days can be determined as parameter c_d in the stage of daily collision analysis together with other orbit parameters, 2−3 days after risk object is proposed. In the stage of precision collision warning, based on more measurement orbit data, the error can be further corrected dynamically. Meanwhile, the influence of solar $F_{10.7}$ flows and its changes in 24 hours on atmospheric density is mainly reflected in the process in atmospheric heating. Studies show that its influence on atmospheric density will be delayed in 24 hours. In the prediction of orbit determination, as long as the quasi-real-time measured data of $F_{10.7}$ are acquired, its effect on orbit position prediction in 24 hours can be ignored. Therefore the impact of the first three factors on orbit prediction in 24 hours can be reduced to the minimum. However, for the fourth factor geomagnetic index, its impact on orbit prediction in 24 hours cannot be corrected by c_d. Especially, if there is significant geomagnetic storm in 24 hours, the accuracy of orbit prediction in 24 hours will decrease by an order of magnitude.

Through researches scientists found that before geomagnetic storms, there must be an intense solar storm erupting from sunspot 24−48 hours ahead. Therefore by observing the sun, it can be predicted whether there will be an anomaly jump of geomagnetic index. The

probability of the occurrence of this kind of anomaly jump in a year is no greater than 10%. That is to say, for red warning released 24 hours before intersection, in 90% cases, orbit prediction error caused by the uncertainty of atmospheric drag perturbation model can be controlled within a certain range. Therefore collision warning threshold can be set according to different orbital altitudes of space objects. In the process, special attention should be paid to the pattern that orbit precision in radial and normal direction is higher than that in tracking direction.

With appropriate threshold in radial direction, most of the false alarms in yellow warnings can be removed effectively. Red warning released in this case is highly credible. For space objects of normal size, the probability of collision is generally higher than 10^{-4} in red warning, meaning that there would be a real collision event among 10,000 times of red warning. However, given the very serious damage of collision, to guarantee complete safety, we recommend that the work of avoidance control can be carried out for space objects with the ability of on-orbit maneuvers, especially for manned spacecraft or spacecraft with high values. Indicated by sunspots observation and the calculation of c_d, if a geomagnetic storm may occur in the next 24−48 hours or the red warning is in the period of a geomagnetic storm, proving that the confidence level of the red warning is lower, then avoidance control can be decided whether to be carried out based on the calculated probability of collision warning and the maximum probability comprehensively.

The accuracy of orbit prediction is higher if red warning is released near the collision point, giving a higher credibility. However, the preparation procedure of space object orbit control requires relatively longer time. In addition, theoretically, fuel consumption will be less if orbit control is carried out earlier, whereas the result of avoidance control is better. Therefore from this point of view, it is better to carry out the avoidance control earlier. Considering the controllable 24-hours atmospheric drag model errors and the feasibility of intensive observations of detection network, red warning is suggested to be released 24 hours in advance of a potential collision.

6.3.4 Avoidance control

The procedure of avoidance control starts 24 hours before the collision. Generally, avoidance control should be carried out 6 hours before collision. First, based on the theoretical postcontrol orbit, collision warning analysis of spacecraft orbit in the next 3 days after the avoidance control will be made so that safety assessment of postcontrol could be carried out. If a yellow warning event exists, recalculate the theoretical postcontrol orbit. Repeat the process, until there will be no yellow warning event.

The selection of orbit avoidance strategy is related to the capacities and status of spacecraft control components in each direction, as well as the orbit control decision-making capability of spacecraft management department. In most cases the follow-up tasks of spacecraft should also be considered in the process of the above choice. Accordingly, the selection of orbit avoidance strategy is often a complex process. Altitude avoidance method and time avoidance method given in Section 6.2 are two typical algorithms. For both algorithms, the theoretical postcontrol orbit must be analyzed to ensure that there would not be any new risks.